Evolutionary Systematics. 10 2026, 31–46 | DOI 10.3897/evolsyst.10.172168

PENSOFT

EVOLUTIONARY SYSTEMATICS

Integrative taxonomy unveils a new lineage within *Acanthogonatus centralis* Goloboff, 1995 (Araneae, Mygalomorphae, Pycnothelidae): description of *Acanthogonatus monicae* sp. nov. from central Argentina

Fiorella Signorotto[1], Nelson Ferretti[1]

1 *Centro de Recursos Naturales Renovables de la Zona Semiárida (CERZOS-UNS, CONICET), Camino La Carrindanga, km.7, Bahía Blanca (8000), Buenos Aires, Argentina*

https://zoobank.org/644FA930-70A4-4E02-A647-FFE90F2F6926

Corresponding author: Fiorella Signorotto (fsignorotto@cerzos-conicet.gob.ar)

Academic editor: Stephanie F. Loria ♦ **Received** 18 September 2025 ♦ **Accepted** 3 February 2026 ♦ **Published** 12 February 2026

Abstract

A new species of Pycnothelidae Chamberlin, 1917 from the Pampean mountain ranges, Córdoba, Argentina is described and illustrated: *Acanthogonatus monicae* **sp. nov.** Here, we combine morphological analyses, molecular phylogeny based on the COI gene, species delimitation methods (bPTP, ABGD), and ecological niche modeling. These approaches consistently support two independent evolutionary lineages previously assigned to *A. centralis* Goloboff, 1995. The new species is morphologically similar to *A. centralis* and *A. parana* Goloboff, 1995, but differs from both by genitalic characters in males and females. Additionally, an updated identification key for Argentine species of *Acanthogonatus* is provided.

Key Words

Ecological niche modeling, phylogeny, Pycnothelidae, South America

Introduction

Recent molecular studies have revalidated the family status Pycnothelidae Chamberlin, 1917 within Mygalomorphae, separating it from many subfamilies formerly included in Nemesiidae Simon, 1889 (Opatova et al. 2019; Montes de Oca et al. 2022). Currently, the family comprises 15 genera and 140 valid species (Montes de Oca et al. 2022; World Spider Catalog 2025). Its geographic distribution includes Africa, Australasia and South America (Opatova et al. 2019), and its members are nocturnal spiders that usually construct open burrows, sometimes with surface extensions (Opatova et al. 2019). Members of this family can be recognized by the following morphological characteristics: (i) presence of an intercheliceral tumescence in males, ranging in size from small to large and typically pale yellow in color, covered with few to numerous setae; (ii) absence of dorsal spines on the male palpal cymbium; (iii) leg III patella with a 1–1–1 prolateral spine arrangement; (iv) flexible tarsi in one or more legs of males; (v) tarsal organ located at the central apical region; and (vi) absence of claw tufts (Goloboff 1995; Montes de Oca et al. 2022).

The most diverse Neotropical genus within Pycnothelidae is *Acanthogonatus* Karsch, 1880, which currently includes 30 described species (World Spider Catalog, 2025). The type species is *A. franckii* Karsch, 1880 from Chile. In Argentina, the following species have been recorded: *A. birabeni* Goloboff, 1995; *A. centralis* Goloboff, 1995; *A. confusus* Goloboff, 1995; *A. fuegianus* Simon, 1902; *A. messii* Signorotto & Ferretti, 2023; *A. notatus* Mello-Leitão, 1940; *A. parana* Goloboff, 1995; and *A. patagonicus* Simon, 1905 (Catálogo de Arañas de Argentina 2025; World Spider Catalog 2025).

Goloboff (1995) studied the phylogenetic relationships within *Acanthogonatus* and relatives, based on representatives from Argentina, Chile, Peru, and Uruguay. He proposed four species groups: the *nahuelbuta*, *mulchen*,

Copyright *Fiorella Signorotto & Nelson Ferretti.* This is an open access article distributed under the terms of the Creative Commons Attribution License (CC BY 4.0), which permits unrestricted use, distribution, and reproduction in any medium, provided the original author and source are credited.

franckii, and *patagonicus* species groups. However, three Argentinean species (*A. centralis*, *A. parana*, and *A. confusus*) could not be placed within any of these groups, despite being described in the same study.

Acanthogonatus centralis Goloboff, 1995 is a species commonly found in the mountainous systems of central Argentina, including southern Buenos Aires province, western Córdoba, central San Luis, and eastern San Juan provinces (Goloboff 1995). It is a medium-sized spider, with both males and females reaching approximately 12 mm in total body length (Ferretti et al. 2011). These spiders construct dense, unbranched silk tubes with a single open entrance (Ferretti et al. 2011). Males exhibit two distinct peaks of activity during spring and late autumn (Ferretti et al. 2012). They display a generalist diet (Pompozzi and Copperi 2018). Their foraging strategy is passive, waiting for prey at the tube entrance, a behavior characteristic of mygalomorph spiders (Coyle 1990). Males of this species are characterized by smooth palpal bulb with no keels and a well-developed tibial apophysis bearing two short, stout spines, females are characterized by spermathecae with an oval-shaped receptacle bearing a blunt apex and an internal projection shorter than the receptacle itself (Goloboff 1995).

Calatayud-Mascarell et al. (2022) investigated the phylogeographic patterns of *A. centralis* across the peripampasic mountainous systems from central Argentina. Their study revealed significant genetic structuring among the populations from the Ventania mountainous system (Buenos Aires Province) and those from the Pampean ranges (Córdoba Province), with divergence times estimated at about 3–5 million years ago (Pliocene). This study relied only on a fragment of the mitochondrial 16S rRNA gene (16S), which should be treated with caution for species delimitation or barcoding when using small fragments (500 bp) instead of the large fragments of about 1500 bp (Chan et al. 2022), or additional nuclear loci. Although the 16S gene has been demonstrated to be superior to the universal cytochrome *c* oxidase subunit 1 (CO1) barcoding gene for phylogenetic estimation of many animals (Hertwig et al. 2004; Vences et al. 2012), its superiority over CO1 with regard to non-phylogenetic inferences such as species identification/delimitation is less clear. Indeed, many studies showed that CO1 outperforms 16S in species identification (Xia et al. 2012; Rockney et al. 2015). In this context, the present study aims to test the species boundaries of *A. centralis* from two disjunct mountainous systems by integrating multiple lines of evidence, such as morphological, molecular, and ecological niche data. In particular, we incorporate analyses of the COI gene, which offers reliable resolution for elucidating intraspecific relationships and identifying potential independent evolutionary lineages. We propose the designation of a new *Acanthogonatus* species that belong to the individuals from populations of Córdoba mountain ranges.

Methods

Material examined and study area

In this study, we examined specimens from the arachnological collection of CERZOS-CONICET (UNS, Bahía Blanca), collected during field campaigns in central Argentina since 2009. In addition, the type material deposited at the Museo Argentino de Ciencias Naturales "Bernardino Rivadavia" (MACN) was examined. The material was used for morphological and molecular analyses, focusing on *A. centralis* populations from two mountain systems: Ventania (Buenos Aires) and the Pampean Mountains (Córdoba) (Fig. 1).

Specimens used for morphological studies. *Acanthogonatus centralis*. ARGENTINA • Holotype. 1 ♂; Buenos Aires, Sierra de la Ventana, between Pringles and Saavedra; 26–29 Aug. 1987; P. Goloboff leg.; MACN-Ar 48890

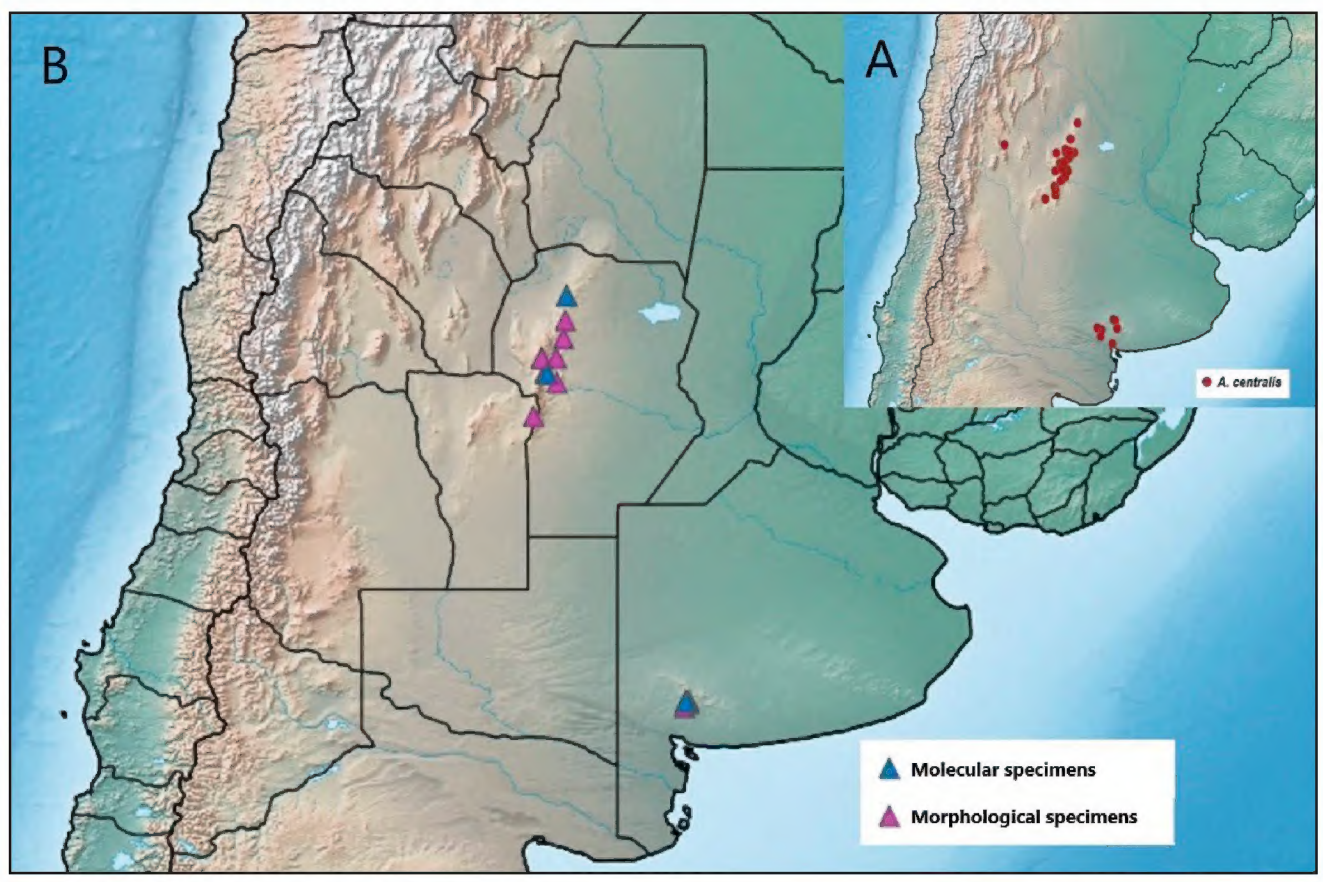

Figure 1. Distribution of *Acanthogonatus centralis*. **A.** Map showing the known localities of *A. centralis* prior to species delimitation, including both populations; **B.** Map showing the localities where material was collected for morphological and molecular analyses.

• Paratype. 1 ♀; same data as holotype; MACN-Ar 48915 • 1 ♀, Córdoba, Santa Rosa de Calamuchita; 32.07720°S, 64.53980°W; Feb. 2017; N. Ferretti leg.; M1507 • 1 ♀, Córdoba, Ascochinga; 30.94220°S, 64.27610°W; Feb. 2017; N. Ferretti leg.; M1498 • 1 ♀, Córdoba, Camino del Cuadrado; 31.12861°S, 64.40299°W; Feb. 2017; N. Ferretti leg.; M1508 • 1 ♀, Córdoba, El Cóndor; 31.63783°S, 64.67997°W; Feb. 2017; N. Ferretti leg.; M1503 • 1 ♀, Córdoba, La Cumbrecita; 31.90932°S, 64.76510°W; Feb. 2017; N. Ferretti leg.; M1506 • 1 ♀, Córdoba, Observatorio; 31.58650°S, 64.51630°W; Feb. 2017; N. Ferretti leg.; M1501 • 1 ♂, Córdoba, El Cóndor; 31.63783°S, 64.67997°W; Feb. 2017; N. Ferretti leg.; M1495 • 1 ♂, Córdoba, Alpa Corral; 32.68949°S, 64.73351°W ; Feb. 2017; N. Ferretti leg.; M1496 • 1 ♂, Córdoba, El Cóndor; 31.63783°S, 64.67997°W; Oct. 2013; N. Ferretti & M.S. Copperi leg.; M0427 • 1 ♀, Buenos Aires, Sierra de la Ventana; 38.12786°S, 61.78944°W; Oct. 2009; N. Ferretti, G. Pompozzi & M.S. Copperi leg.; M205 • 1 ♀, Buenos Aires, Parque Tornquist; 38.06696°S, 61.98005°W; Jul. 2019; N. Ferretti, G. Pompozzi, M.S. Copperi & L. Schwerdt leg.; M0905 • 1 ♀, Buenos Aires, Parque Tornquist; 38.06696°S, 61.98005°W; Sept. 2009; N. Ferretti, G. Pompozzi & M.S. Copperi leg.; M0170 • 1 ♀, Buenos Aires, Parque Tornquist; 38.06696°S, 61.98005°W; Sept. 2010; N. Ferretti, G. Pompozzi & M.S. Copperi leg.; M0505 • 1 ♀, Buenos Aires, Funke; 38.07226°S, 62.05308°W; Apr. 2009; N. Ferretti & G. Pompozzi leg.; M0089 • 1 ♂, Buenos Aires, Funke; 38.07226°S, 62.05308°W; Apr. 2012; N. Ferretti, G. Pompozzi, M.S. Copperi & L. Schwerdt leg.; M0951 • 1 ♂, Buenos Aires, Parque Tornquist; 38.06696°S, 61.98005°W; Sept. 2010; N. Ferretti, G. Pompozzi & M.S. Copperi leg.; M0509.

Specimens used for molecular studies. *Acanthogonatus centralis*. Argentina • 2 ♂♂, Córdoba, Villa Berna; 31.90989°S, 64.73926°W; Feb. 2017; N. Ferretti leg.; GIASF1/2 • 2 ♂♂, Córdoba, Dean Funes; 30.43250°S, 64.26551°W; Feb. 2017; N. Ferretti leg.; GIASF3/4 • 2 ♂♂, Buenos Aires, Funke; 38.07226°S, 62.05308°W; Feb. 2017; N. Ferretti leg.; GIASF5/6.

List of abbreviations

ALE, anterior lateral eyes; **AME**, anterior median eyes; **Cy**, cymbium; **d**, dorsal; **MACN**, Museo Argentino de Ciencias Naturales "Bernardino Rivadavia"; **PLE**, posterior lateral eyes; **PLS**, posterior lateral spinnerets; **PME**, posterior median eyes; **PMS**, posterior median spinnerets; **p**, prolateral; **pt**, prolateral teeth; **r**, retrolateral; **Ti**, tibia; **v**, ventral.

Morphological characters

Morphological terminology follows Goloboff (1995) and Indicatti et al. (2015), and spine notation follows Petrunkevitch (1925). Measurements are in millimeters (to 0.01 mm) using a Prec. Measuring© digital caliper. Total body length includes carapace and abdomen, excluding chelicerae, pedicel, and spinnerets. Male palpal bulbs were removed with entomological forceps and photographed with an MShot digital camera on a Leica S APO stereomicroscope in four standard views (dorsal, prolateral, retrolateral, ventral), using focus stacking of 10 planes processed with HELICON FOCUS v.7. Female spermathecae were dissected with entomological scissors, cleared with Naclens© enzyme solution (24 h in distilled water), and photographed in dorsal view.

Molecular characters

DNA was obtained from leg III tissues of six individuals from both populations. Extractions and isolation of DNA were made at the Genomic Services Laboratory (GENeTyC) from CERZOS-UNS. DNA was amplified via polymerase chain reaction (PCR) using the following protocol: 94 °C for 9 min, then 34 cycles of 94 °C 45 s; annealing 48◦C 45 s; 72◦C 60 s; with a final elongation step of 72 °C for 6 min. We used a single set of primers to amplify the barcode region of mitochondrial COI gene: LCO-1490 (5′-GGTCAACAAATCATAAAGATATTGG-3′) and HCO-2198 (5′- TAAACTTCAGGGTGACCAAAAAATCA-3′) (Folmer et al. 1994). Sequencing was carried out in Macrogen (Korea) and the edition was made using the software GENEIOUS R11. Alignments were performed with the MAFFT v.7308 plugin implemented in GENEIOUS. Additionally, sequences of related taxa were downloaded from GenBank to be used as outgroups (Table 1).

Table 1. Samples used for molecular analyses. Collection codes, localities, and GenBank accession numbers. B.A. Buenos Aires; C = Catamarca; Cba = Córdoba.

Species	Code	Locality	GenBank Accession Number
Acanthogonatus sp.	GIASF1	Villa Berna Cba.	PX935567
Acanthogonatus sp.	GIASF2	Villa Berna Cba.	PX935568
Acanthogonatus sp.	GIASF3	Dean Funes Cba.	PX935570
Acanthogonatus sp.	GIASF4	Dean Funes Cba.	PX940743
A. centralis	GIASF5	Funke B.A.	PX935571
A. centralis	GIASF6	Funke B.A.	PX935569
Grammostola vachoni	-	Tandil B.A.	PV644568.1
Plesiopelma absconditus	-	El singüil C.	PP028763.1
A. campanae	-	-	KY017803.1
Nemesia pannonica	-	-	KX039280.1
Nemesia sp.	-	-	MT607825.1

Phylogenetic analyses

The molecular data matrix was analyzed using Bayesian Inference (BI) and Maximum Likelihood (ML) approaches. PARTITIONFINDER v.2.1.1 (Lanfear et al. 2016) was employed to determine the optimal partitioning scheme and evolutionary model based on an initial

configuration by codon position (for coding genes). The most appropriate model according to PartitionFinder was TIM+F for the three codon positions. BI analyses were conducted in MRBAYES v.3.2.6 (Ronquist and Huelsenbeck 2003), and ML analyses were performed using IQ-TREE v.1.6.12 (Nguyen et al. 2015). Resampling methods were applied to estimate nodal support (bootstrap for ML and posterior probabilities for BI). Finally, resulting trees were visualized and edited with FIGTREE v1.4.2.

Lineage delimitation

This study applies the unified species concept (de Queiroz 2007), combining morphological analysis with molecular approaches: Automatic Barcode Gap Discovery (ABGD, distance-based) and Bayesian Poisson Tree Processes (bPTP, tree-based), excluding outgroups to improve results (Zhang et al. 2013). Candidate species were considered valid when consistently recovered across analyses, minimizing overestimation in cases of discrepancy.

Ecological niche modeling

Niche overlap was assessed among the closely related lineages using ecological niche models generated in MAXENT v3.3.3 (Phillips et al. 2009), followed by replicated models for each species based on occurrence records from the arachnological collection of CERZOS-CONICET, UNS, and published sources (Goloboff 1995; Ferretti et al. 2014). Models with the highest Area Under the Curve (AUC) of the Receiver Operating Characteristic (ROC) curve were selected (Pearson et al. 2007), considering values > 0.8 as "good" and > 0.9 as "highly accurate" (Luoto et al. 2005). Present-day (1950–1999) and past (Pliocene) climate layers were obtained from WorldClim (worldclim.org) and ecoClimate (Lima-Ribeiro et al. 2015). Of the 19 initial bioclimatic variables, those with correlation coefficients > 0.8 were excluded (Jezkova et al. 2011) using ENMTools v1.4.4 (Warren 2010), retaining six variables for final modeling: BIO2 (Mean Diurnal Range), BIO3 (Isothermality, calculated as (BIO2 / BIO7) × 100), BIO4 (Temperature Seasonality, expressed as the standard deviation of monthly temperature values × 100), BIO15 (Precipitation Seasonality, defined as the coefficient of variation of monthly precipitation), BIO18 (Precipitation of the Warmest Quarter), and BIO19 (Precipitation of the Coldest Quarter).

Results

Molecular phylogeny

The tree, rooted with sequences from *Grammostola* Simon, 1892 and *Plesiopelma* Pocock, 1901, showed similar topologies in BI and ML, with different levels of support (Fig. 2). Nemesiidae (*Nemesia* sp. and *N. pannonica* Herman, 1879) was recovered as sister to Pycnothelidae, a clade that included all *Acanthogonatus* sequences used in this study. Within this clade, *A. campanae* was recovered as sister to *A. centralis*, and two independent lineages of *A. centralis* were also recovered: one from the Ventania mountain range (Funke) and another from Córdoba (Dean Funes and Villa Berna).

Species delimitation

Two different species delimitations were obtained in relation to the method applied. The bPTP analysis split the species into two lineages: one corresponding to the population from the Ventania mountain range, and the other grouping the representatives from the central-northern mountain ranges of Córdoba, without further differentia-

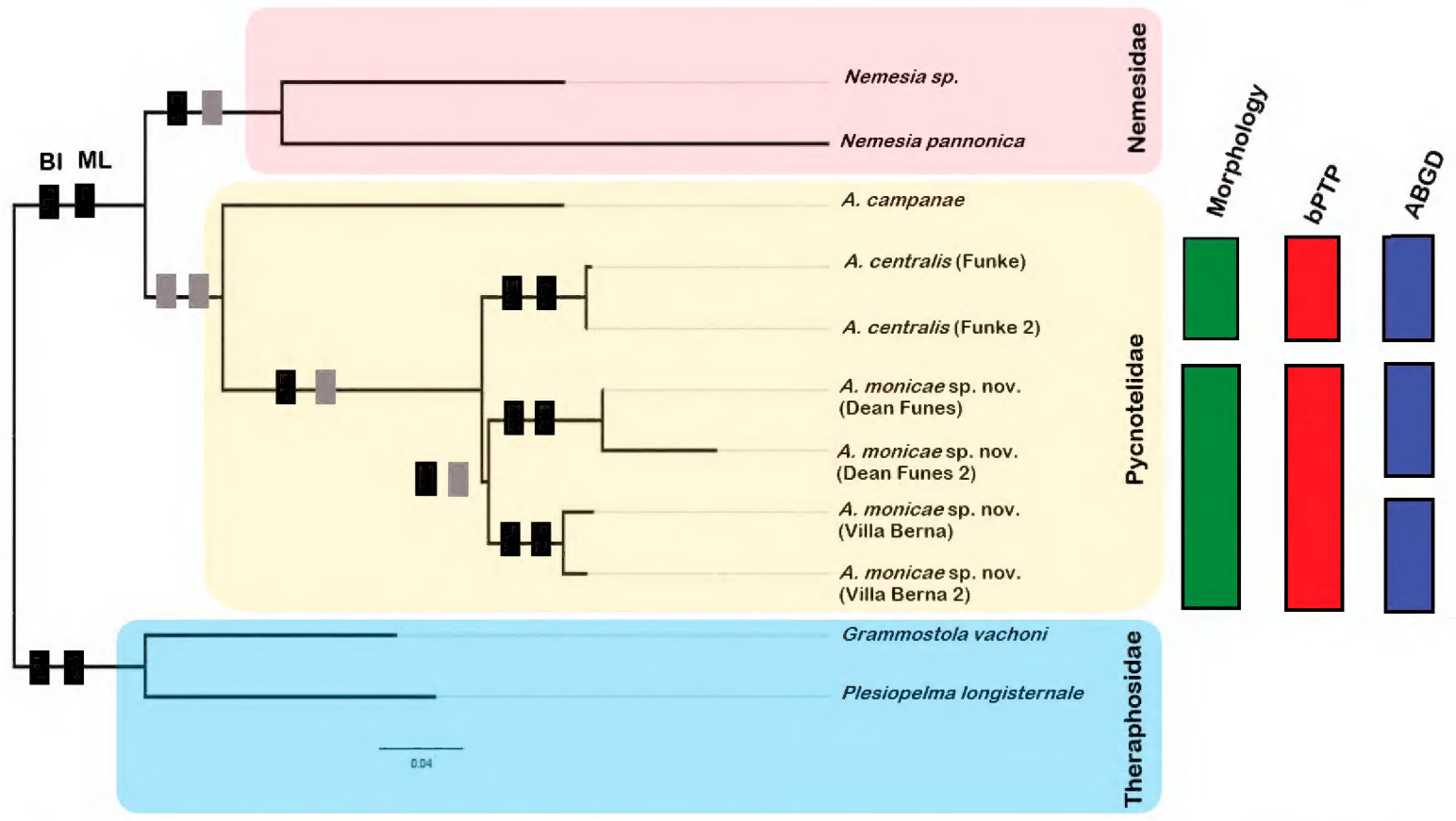

Figure 2. Phylogenetic tree obtained using Bayesian Inference (BI) and Maximum Likelihood (ML) methods. Node support is indicated by black squares (>70) and grey squares (<70) for both models. Lineages identified through species delimitation approaches (Morphology, bPTP, ABGD) are highlighted with colored boxes.

tion among those populations (Fig. 2). The ABGD method identified three possible lineages: one corresponding to the Ventania range in Buenos Aires, and two within the central-northern ranges of Córdoba, distinguishing a lineage in the central part of the province (Villa Berna) and another in the northern populations (Dean Funes) (Fig. 2).

Ecological niche modeling

Based on current climatic conditions, the predictive model for *A. centralis* from the Ventania mountain range reached an AUC value of 0.937. The most relevant variable was BIO4 (temperature seasonality), together with BIO3 (isothermality), which jointly accounted for 91.3% of the prediction (Table 2). The predicted current distribution for this population mainly covers the western part of Buenos Aires province, extending into eastern La Pampa and southern Córdoba (Fig. 3A, B).

Table 2. Percentage contribution of the most important bioclimatic variables to the distribution models of *A. centralis* (south-central) and *Acanthogonatus monicae* (central-northern). Values are expressed as percentages. Asterisks (*) indicate the variables with the highest contribution.

	Bioclimatic variables					
Model	BIO2	BIO3	BIO4	BIO15	BIO18	BIO19
A. centralis	-	36.8*	54.5*	0.8	4.5	3.4
A. monicae	1.8	-	29.4*	26.7*	14.7	27.3*

During the Pliocene, the specific model for this population yielded an AUC of 0.938, where BIO4 was again the most important variable, contributing 96.3%. At that time, the most suitable areas were located primarily in the south-central region of Buenos Aires, with extensions into northwestern La Pampa and a smaller zone in northern Río Negro (Fig. 4C).

The current predictive model for *A. monicae* sp. nov. from the central-northern mountains of Córdoba

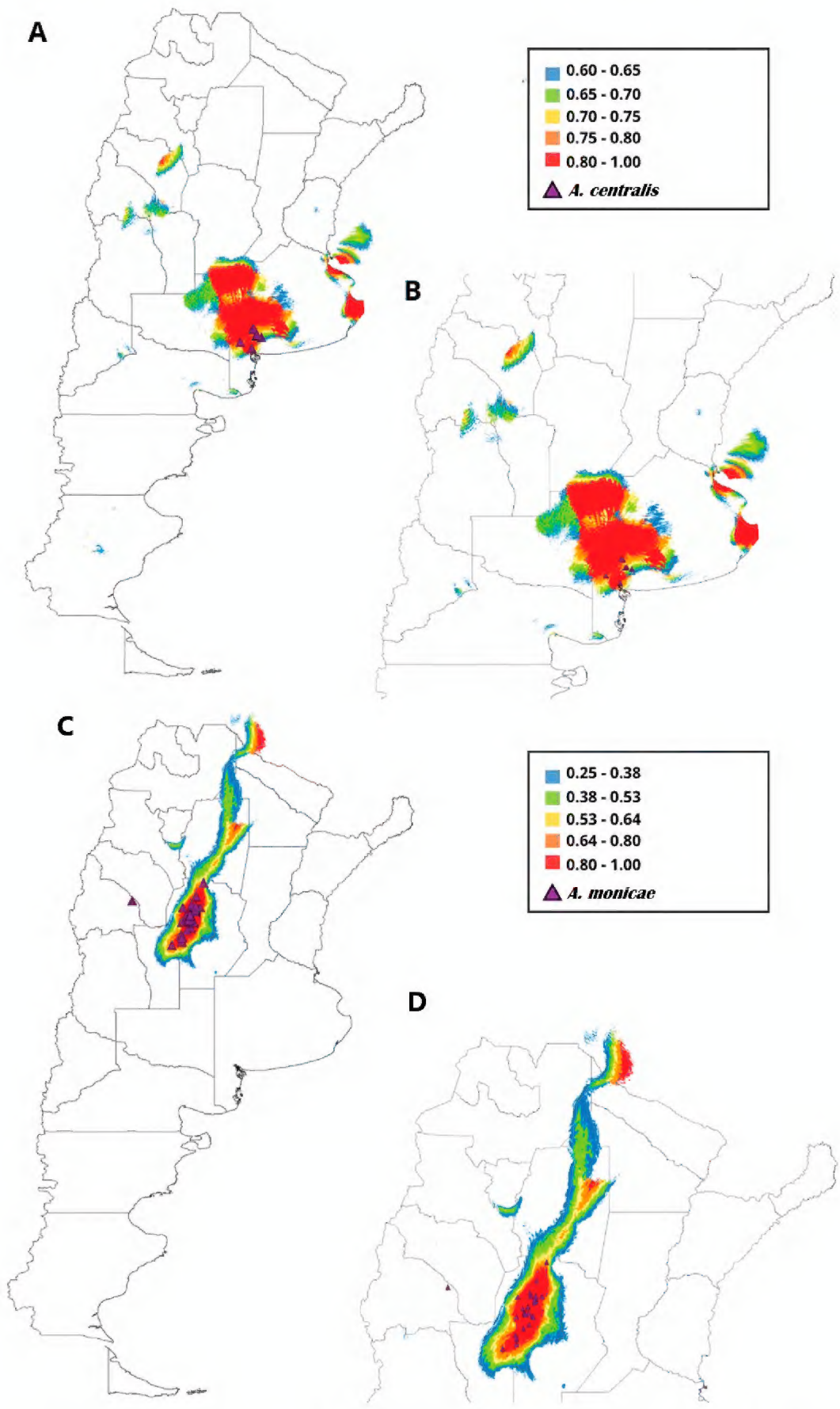

Figure 3. Ecological niche model under current climatic conditions. **A, B.** *A. centralis*; **C, D.** *A. monicae*. Colours indicate habitat suitability from low (blue) to high (red), while violet triangles represent occurrence records for each species.

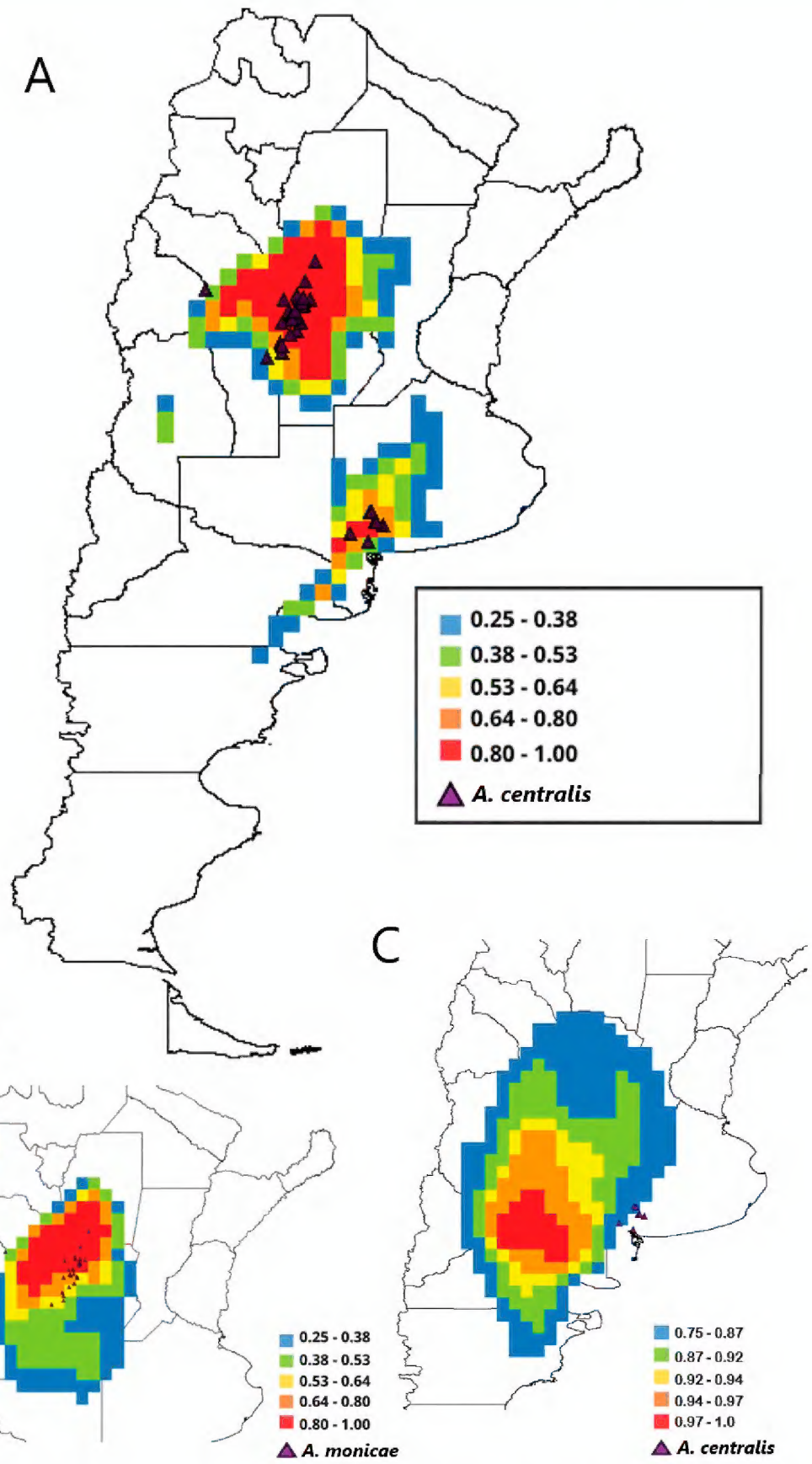

Figure 4. Niche modeling of *Acanthogonatus centralis* under Pliocene climatic conditions. **A.** Initial general model prior to species delimitation, including both populations; **B.** central-northern population (*A. monicae*); **C.** Central-southern population (*A. centralis*). Colours indicate habitat suitability from low (blue) to high (red), while violet triangles represent occurrence records for each species.

achieved an AUC of 0.980. The main contributing variable was BIO4 (temperature seasonality), accompanied by BIO19 (precipitation of the coldest quarter) and BIO15 (precipitation seasonality), which together explained 83.3% of the prediction (Table 2). Suitable areas for the current distribution include northeastern Córdoba, northwestern San Luis, central Santiago del Estero, and western Chaco, mainly associated with the dry Chaco ecoregion (Fig. 3C, D).

The Pliocene model for this population yielded an AUC value of 0.989, with BIO4 contributing 67.1% and BIO19 contributing 19%. During this period, the most favorable areas shifted northward compared to their current distribution, mainly encompassing Córdoba province and partially extending into San Luis, Santiago del Estero, and La Rioja (Fig. 4B).

The predictive model for all *A. centralis* northern and southern populations during the Pliocene, based on ecoclimate variables, yielded an AUC value of 0.988. BIO4 (temperature seasonality) was the main contributing variable, accounting for 78.3%. The highest suitability areas were located in southern Buenos Aires and the central-northern region of Córdoba province, extending towards La Rioja, San Juan, and San Luis (Fig. 4). No overlap was observed between the high-probability areas for the northern and southern populations.

Taxonomy

Order Araneae Clerck, 1757
Family Pycnothelidae Chamberlin, 1917

Genus *Acanthogonatus* Karsch, 1880

Acanthogonatus Karsch, 1880: 391.

Tryssothele Simon, 1902: 7. Type species *Tryssothele fuegiana* Simon, 1902, by original designation. Synonymised by Raven, 1985:83.

Chubutia Mello-Leitão, 1940: 3. Type species *Chubutia notata* Mello-Leitão, 1940, by original designation. Synonymised by Schiapelli & Gerschman, 1970: 152.

Type species. *Acanthogonatus francki* Karsch (1880), by original designation.

Species included. *Acanthogonatus alegre* Goloboff, 1995; *A. birabeni* Goloboff, 1995; *A. brunneus* Nicolet, 1849; *A. campanae* Legendre & Calderón, 1984; *A. centralis* Goloboff, 1995; *A. chilechico* Goloboff, 1995; *A. confusus* Goloboff, 1995; *A. ericae* Indicatti, Lucas, Ott & Brescovit, 2008; *A. francki* Karsch, 1880; *A. fuegianus* Simon, 1902; *A. hualpen* Goloboff, 1995; *A. huaquen* Goloboff, 1995; *A. incursus* Chamberlin, 1916; *A. juncal* Goloboff, 1995; *A. messii* Signorotto & Ferretti, 2023; *A. minimus* Indicatti, Folly-Ramos, Vargas, Lucas & Brescovit, 2015; *A. mulchen* Goloboff, 1995; *A. nahuelbuta* Goloboff, 1995; *A. notatus* Mello-Leitão, 1940; *A. parana* Goloboff, 1995; *A. patagallina* Goloboff, 1995; *A. patagonicus* Simon, 1905; *A. peniasco* Goloboff, 1995; *A. pissii* Simon, 1889; *A. quilocura* Goloboff, 1995; *A. recinto* Goloboff, 1995; *A. subcalpeianus* Nicolet, 1849; *A. tacuariensis* Pérez-Miles & Capocasale, 1982; *A. tolhuaca* Goloboff, 1995; *A. vilches* Goloboff, 1995; *A. monicae* sp. nov.

Identification key for *Acanthogonatus* Karsch, 1880 updated from Signorotto et al. (2023)

Males

Males of *A. alegre* Goloboff, 1995, *A. brunneus* (Nicolet, 1849), *A. incursus* (Chamberlin, 1916), *A. juncal* Goloboff, 1995, *A. mulchen* Goloboff, 1995, *A. parana* Goloboff, 1995, *A. peniasco* Goloboff, 1995, *A. tolhuaca* Goloboff, 1995 and *A. vilches* Goloboff, 1995 are unknown.

1 ITC IV absent 2
– ITC IV present 17
2 Apophysis with two apical laminar spines on the same base; palpal tibia with two dorsal sinuous long setae; bulb with no keels, or with lateral keels 3
– No tibial apophysis of any kind; ITC I absent; forests in southern Chile and Argentina ..... *A. confusus* Goloboff, 1995
3 Bulb with a lateral keel forming a concavity (Goloboff 1995: fig. 81B, C in); central Chile (regions IV, V) ..... *A. huaquen* Goloboff, 1995
– Bulb different 4
4 Dorsal abdomen yellowish with a chevron; apical article of PLS short, triangular; Argentina (dry regions of Patagonia) and southern Chile 5
– Dorsal abdomen with pattern formed by numerous mottles; apical article of PLS longer, digitiform; Argentina (north of Patagonia) 9
5 Large spiders (about 20 mm total length, carapace over 9 mm; bulb with two lateral flanges delimiting concave triangular area; palpal tibia rather elongate (Goloboff 1995: fig. 98B) ..... *A. patagonicus* (Simon, 1905)
– Medium to small spiders (total length 15 mm or smaller, carapace below 6 mm); bulb variable; palpal tibia shorter .. 6
6 Bulb with low lateral keels (or with single keel); metatarsi I with at least 1 or 2 ventral spines 7
– Bulb with more developed lateral keels (Goloboff 1995: fig. 100C, D) in metatarsi I with no ventral spines ..... *A. notatus* (Mello-Leitão, 1940)
7 Bulb with a single keel; patella III with 1-1-1 P 8
– Bulb with a double keel (Goloboff 1995: fig. 101A, B); in patella III with only 0-0-1; slightly larger (carapace length about 5 mm) ..... *A. chilechico* Goloboff, 1995
8 Bulb with slightly developed keel (Goloboff 1995: fig. 102A, B), maxillae without cuspules.... *A. birabeni* Goloboff, 1995
– Bulb with well-developed keel (Signorotto et al. 2023: fig. 4A–D), maxillae with more than 15 cuspules ..... *A. messii* Signorotto & Ferretti, 2023
9 Dorsal abdomen blackish with yellowish whitish oblique lines; bulb with widened, flanged tip (Goloboff 1995: fig. 87B); extremely common in central-southern Chile (regions IV-VIII) ..... *A. pissii* (Simon, 1889)
– Dorsal abdomen with only white dots not forming continuous lines, or mottled; bulb with narrower tip, flanged in the base or without flanges 10
10 Bulb with no keels; total length c. 13 mm; central Argentina (Córdoba, San Luis, San Juan, and Buenos Aires)..... 11
– Bulb with serrated, curved and long embolus; central Chile, Uruguay and southern Brazil 12
11 Palpal bulb bearing 7 subapical prolateral teeth (Fig. 5A–D) ..... *A. centralis* Goloboff, 1995
– Palpal bulb with very thin embolus, straight in dorsal view, bearing 8–10 subapical teeth (Fig. 8A–G) ..... *A. monicae* Signorotto & Ferretti, sp. nov.
12 Metatarsus I slightly curved downward (Montenegro and Aguilera 2024: fig. 2h); central Chile... *A. quilocura* Goloboff, 1995
– Metatarsus I straight 13
13 Presence of flanges along the embolus..... 14
– Absence of flanges on embolus 15

14 One flange on palpal embolus apex (Indicatti et al. 2008: figs 20, 21); southern Brazil . *A. ericae* Indicatti, Lucas, Ott & Brescovit, 2008
– Bulb with three perpendicular flanges along embolus (Goloboff 1995: fig. 95D, E) ..... *A. francki* Karsch, 1880
15 Bulb with a winglike projection (Goloboff 1995: fig. 96D); PLS apical segment digitiform..... *A. recinto* Goloboff, 1995
– Bulb different; PLS apical segment triangular 16
16 Presence of tibial spur on tibia I (Pérez-Miles and Capocasale 1982: figs 5, 6); Uruguay and southern Brazil .... *A. tacuariensis* (Pérez-Miles & Capocasale, 1982)
– Absence of tibial spur on tibia I; Argentina (Patagonia) ..... *A. fuegianus* (Simon, 1902)
17 Anterior tibia with dense prolateral shield of setae 18
– Anterior tibia without such shield 20
18 Palpal tibia widest in basal third, and then uniformly tapering; retrolateral thicker setae present along apical 2/3 of article 19
– Palpal tibia of uniform width along medial half, more abruptly narrowed in the apical third; retrolateral thicker setae present only on apical third ..... *A. hualpen* Goloboff, 1995
19 Bulb with its basal portion rounded, abruptly tapered to form embolus base; basal portion of the bulb duct strongly sinuous (Goloboff 1995: fig. 108A, B) ..... *A. patagallina* Goloboff, 1995
– Bulb with its basal portion not rounded, tapering more gradually to form embolus base; basal portion of the bulb duct little sinuous (Goloboff 1995: fig. 105E, F) ..... *A. nahuelbuta* Goloboff, 1995
20 Tibia I with a strong apical retrolateral megaspine; palpal bulb with twisted embolus; total length less than 5 mm; Brazil (Rio de Janeiro) (Indicatti et al. 2015: figs 2, 4)..... *A. minimus* Indicatti, Folly-Ramos, Vargas, Lucas & Brescovit, 2015
– Tibia I with no retrolateral megaspine; palpal bulb with slightly curved embolus; total length more than 13 mm..... 21
21 No apophysis on anterior tibia..... *A. confusus* Goloboff, 1995
– Low prolateral tibial apophysis, bearing two spines on common base..... 22
22 Palpi long, about three times of the cymbium length (Goloboff 1995: fig. 79F); embolus c. half-length of palpal bulb (Goloboff 1995: fig. 79G, H)..... *A. subcalpeianus* (Nicolet, 1849)
– Palpi normal, about two times of the cymbium length; embolus c. 2/3 length of palpal bulb (Goloboff 1995: figs 92A, B, 93A, B)..... *A. campanae* (Legendre & Calderón, 1984)

Females

Females of *A. birabeni*, *A. chilechico* and *A. patagallina* are unknown.

1 Claw tufts present; Peru ..... *A. incursus* (Chamberlin, 1916)
– Claw tufts absent 2
2 ITC IV absent 3
– ITC IV present 18
3 Patella IV with 1-1-1 4
– Patella IV with 0-0-1 or (more often) no spines at all 8
4 Spermathecae thick, sclerotized (Goloboff 1995: fig. 97)..... *A. peniasco* Goloboff, 1995
– Spermathecae slightly sclerotized 5
5 Spermathecae cactus like; Argentina 6
– Spermathecae different; Chile 7
6 Spermathecae with oval receptacle, apex blunt, internal projection shorter than receptacle itself (Fig. 5E, F) .... *A. centralis* Goloboff, 1995
– Spermathecae with elongated duct leading to sub-spherical receptacle; internal projection digitiform, as long as or longer than receptacle (Fig. 9F) ..... *A. monicae* Signorotto & Ferretti, sp. nov.
7 Spermathecae with short duct, slightly curved from the internal side (Goloboff 1995: fig. 95A)....*A. francki* Karsch, 1880
– Spermathecae without basal dome, long twisted receptaculum duct (Goloboff 1995: fig. 96A) ...*A. recinto* Goloboff, 1995
8 Apical article of PLS triangular..... 9
– Apical article of PLS longer, digitiform 12
9 Spermathecae branched (bi- or trifurcated) (Goloboff 1995: fig. 99A) ..... *A. fuegianus* (Simon, 1902)
– Spermathecae with a basal mound or protuberance..... 10
10 Small spiders (total length about 12, carapace length 5–6 mm); carapace slightly patterned, with margins and medial line lighter; lateral stripes of dorsal abdominal chevron conspicuous; general coloration yellowish 11
– Larger spiders (total length well over 20 mm, carapace length 10 mm or more); carapace not appreciably patterned; dorsal abdominal pattern limited mostly to cardiac area (Goloboff 1995: fig. 98A); general coloration brown with golden hairs ..... *A. patagonicus* (Simon, 1905)
11 Scopula IV absent ..... *A. messii* Signorotto & Ferretti, 2023
– Scopula IV light (Goloboff 1995: fig. 100A) ..... *A. notatus* (Mello-Leitão, 1940)

12 Spermathecae with a main branch and a lateral secondary internal branch arising from middle of main branch 13
– Spermathecal duct arising from the inner side of basal mound or protuberance 14
13 Main spermathecal branch widened distally, apical area oval-shaped (Fig. 5E, F); central Argentina ..... *A. centralis* Goloboff, 1995
– Main spermathecal branch not widened distally, (Goloboff 1995: fig. 91B) apical area as wide as base; eastern Argentina (Entre Ríos) ..... *A. parana* Goloboff, 1995
14 Dorsal abdomen blackish with yellow-white oblique lines; spermathecae with low basal dome (Goloboff 1995: fig. 86A); central and southern Chile (regions IV–VIII) ..... *A. pissii* (Simon, 1889)
– Dorsal abdomen with white dots or spots not forming continuous lines, or yellowish with darker mottles 15
15 Small spiders (total length about 10 mm, carapace 4 mm or smaller); spermathecae weakly sclerotized, very short duct (Goloboff 1995: fig. 84B); patella III with p0-1-1 spines ..... *A. juncal* Goloboff, 1995
– Larger (total length 20 mm or more, carapace 8 mm or more); patella III with p1-1-1 spines 16
16 Spermathecae with blunt basal mound, and duct strongly curved at the base (Goloboff 1995: fig. 83A) ..... *A. quilocura* Goloboff, 1995
– Spermathecae with basal mound tapering more gradually 17
17 Carapace brownish, dorsal abdomen irregularly mottled; with (weak) rastellum; spermathecae with basal dome narrow, duct strong curvate to inner side (Goloboff 1995: fig. 81A); central Chile ..... *A. huaquen* Goloboff, 1995
– Carapace reddish, dorsal abdomen with oblique lines of dots; rastellum absent 18
18 Spermathecae with short copulatory ducts, arising from basal dome side (Goloboff 1995: fig. 85A); Uruguay and southern Brazil ..... *A. tacuariensis* (Pérez-Miles & Capocasale, 1982)
– Spermathecae with short copulatory ducts, arising from the basal dome apex (Indicatti et al. 2008: fig. 19); southern Brazil ..... *A. ericae* Indicatti, Lucas, Ott & Brescovit, 2008
19 ITC I present 20
– ITC I absent 27
20 Spermathecae very long, twisted (Indicatti et al. 2015: fig. 6); fovea T-shaped (Indicatti et al. 2015: fig. 11); Brazil (Rio de Janeiro) ..... *A. minimus* Indicatti, Folly-Ramos, Vargas, Lucas & Brescovit, 2015
– Spermathecae short, not twisted; fovea normal, procurved 21
21 Spermathecae two wide (but flat) plates 22
– Spermathecae different 23
22 Sternum long (Goloboff 1995: fig. 112C); spermathecae fused, without copulatory duct, with shallow medial notch (Goloboff 1995: fig. 112B) ..... *A. mulchen* Goloboff, 1995
– Sternum normal 24
23 Color uniform blackish; patella III with p0-1-1 spines ..... *A. tolhuaca* Goloboff, 1995
– Color brownish, with mottled abdomen; patella III with p0-1-1 or p1-1-1 spines ..... *A. brunneus* (Nicolet, 1849)
24 Spermathecae strongly sclerotized, with a wide cavity, opening through wide passage 25
– Spermathecae weakly sclerotized, flat and with no appreciable cavity; duct opening not conspicuous 26
25 Spermathecae finger like, strongly curved (Goloboff 1995: fig. 106A–C) ..... *A. nahuelbuta* Goloboff, 1995 & *A. hualpen* Goloboff, 1995
– Spermathecae wider, shaped like two pockets (Goloboff 1995: fig. 109D) ..... *A. vilches* Goloboff, 1995
26 Carapace patterned, legs ringed; spermathecae with short copulatory ducts, arising from the external side of basal dome (Goloboff 1995: fig. 79E) ..... *A. subcalpeianus* (Nicolet, 1849)
– Carapace and legs uniform brown; spermathecae single, undivided (Goloboff 1995: fig. 92C); central Chile (regions IV) ..... *A. campanae* (Legendre & Calderón, 1984)
27 Epigastrium posteriorly produced (Goloboff 1995: fig. 94B); spermathecae long (Goloboff 1995: 94A); northern Chile (Region II) ..... *A. alegre* Goloboff, 1995
– Epigastrium normal; spermathecae shorter (Goloboff 1995: fig. 80A–C); southern Chile (Regions VIII–X) and Argentina (Neuquén) ..... *A. confusus* Goloboff, 1995

Acanthogonatus centralis Goloboff, 1995

Figs 5, 10

Acanthogonatus centralis Goloboff, 1995: 96, figs 9, 77, 78, 89A–F, 90 (♀).
Acanthogonatus centralis Ferretti et al., 2010: 21, figs 29, 30 (♂).
Acanthogonatus centralis Grismado & Goloboff, 2014: 113, figs 10, 11 (♂).

Type material. ***Holotype.*** Argentina • 1 ♂; Buenos Aires, Sierra de la Ventana, between Pringles and Saavedra; 26–29 Aug. 1987; P. Goloboff leg.; MACN-Ar 48890, examined. ***Paratype.*** Argentina • 1 ♀; same data as holotype; MACN-Ar 48915, examined.

Diagnosis. Males of *Acanthogonatus centralis* can be recognized by the palpal bulb without keels bearing seven subapical prolateral teeth (Fig. 5A–D), a characteristic that differentiate it from *A. monicae* sp. nov. in combination with a well-developed tibial apophysis bearing two short and stout spines. Additionally, females differ from *A. monicae* sp. nov. by having spermathecae with

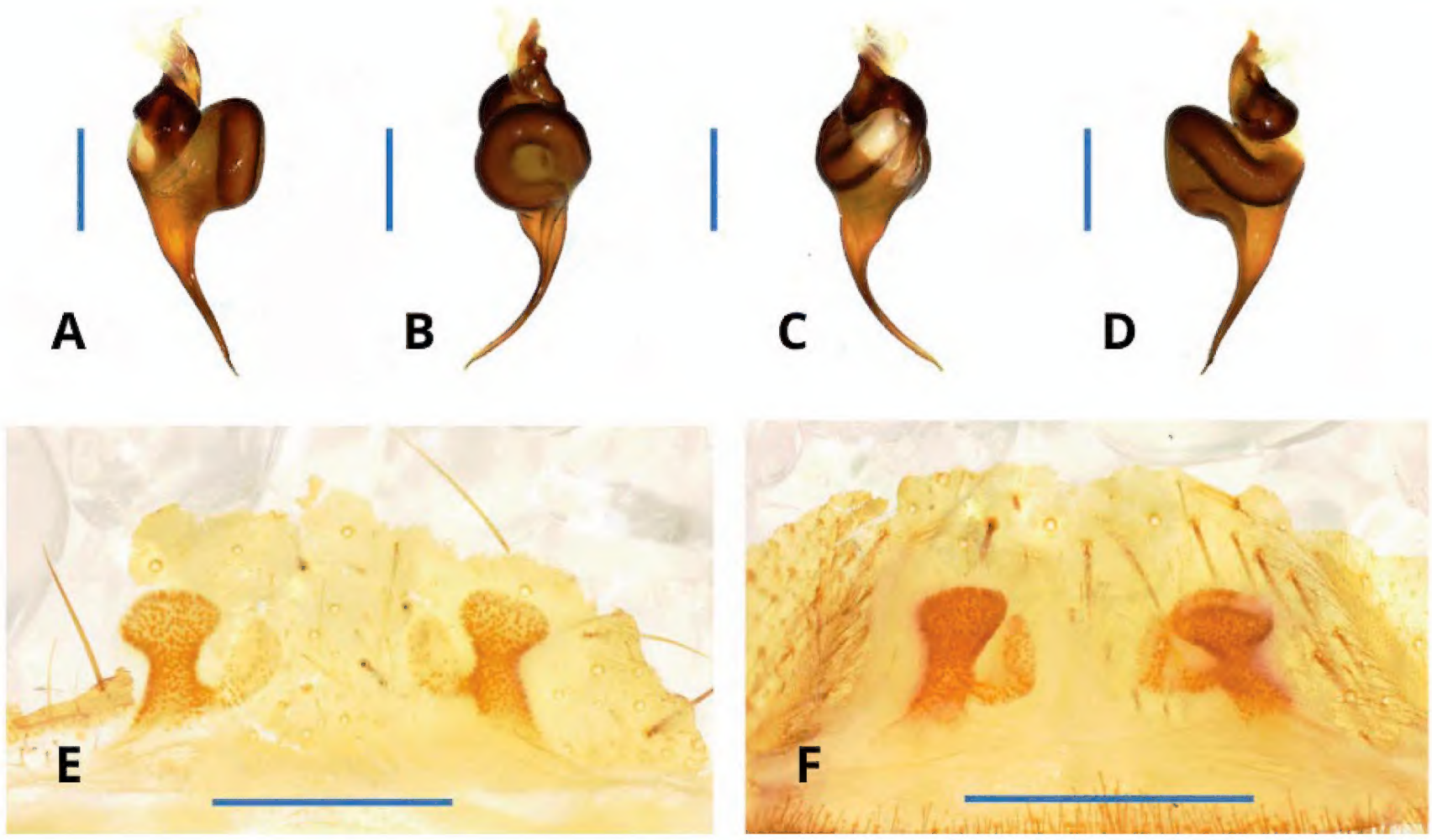

Figure 5. Copulatory organ and spermathecae of *A. centralis*. **A–D.** Male palpal bulbs from Funke locality: **A.** Ventral view; **B.** Retrolateral view; **C.** Prolateral view; **D.** Dorsal view. **E–F.** Females spermathecae, dorsal view: **E.** Female from Tornquist; **F.** Female from Funke. Scale bars: 1 mm.

an oval-shaped receptacle bearing a blunt apex and an internal projection shorter than the receptacle itself. They also differ from *A. parana* by the widened fundus of the spermathecae (Fig. 5E, F).

Description. See Goloboff (1995).

Distribution. Restricted to the south-western mountain ranges of Buenos Aires Province, Argentina (Fig. 10).

Acanthogonatus monicae sp. nov.

https://zoobank.org/F98F7C04-3821-4BA5-8371-392535B4C29C

Figs 6–10

Type material. ***Holotype.*** Argentina • 1 ♂; Córdoba, Alpa Corral; 32.68949°S, 64.73351°W; Feb. 2017; N. Ferretti leg.; M1496. ***Paratype.*** Argentina • 1 ♀; Córdoba, Ascochinga; 30.94220°S, 64.27610°W; Feb. 2017; N. Ferretti leg.; M1498.

Additional material examined. Argentina • 1 ♀; Córdoba, Santa Rosa de Calamuchita; 32.07720°S, 64.53980°W; Feb. 2017; N. Ferretti leg.; M1507 • 1 ♀; Córdoba, Camino del Cuadrado; 31.12861°S, 64.40299°W; Feb. 2017; N. Ferretti leg.; M1508 • 1 ♀; Córdoba, El Cóndor; 31.63783°S, 64.67997°W; Feb. 2017; N. Ferretti leg.; M1503 • 1 ♀; Córdoba, La Cumbrecita; 31.90932°S, 64.76510°W; Feb. 2017; N. Ferretti leg.; M1506 • 1 ♀; Córdoba, Observatorio; 31.58650°S, 64.51630°W; Feb. 2017; N. Ferretti leg.; M1501 • 1 ♂; Córdoba, El Cóndor; 31.63783°S, 64.67997°W; Oct. 2013; N. Ferretti & M.S. Copperi leg.; M0427 • 1 ♂; Córdoba, El Cóndor; 31.63783°S, 64.67997°W; Feb. 2017; N. Ferretti leg.; M1495.

Etymology. The specific name *monicae* is a genitive matronym honoring Mónica, the mother of the first author, in recognition of her constant support and vital role throughout the author's academic journey.

Diagnosis. Males can be distinguished from those of most congeners by the pyriform palpal bulb with a globose tegulum and a long, slender embolus curved prolaterally (Fig. 8A–D) bearing 8 to 10 subapical prolateral teeth (Fig. 8G). They resemble males of *A. centralis*, but differ by the higher number of teeth and a more curved and tapered embolus in dorsal view (Fig. 8C). Females resemble those of *A. centralis* and *A. parana*, but differ from those of *A. centralis* by the spermathecae with an elongated spermathecal duct leading to a sub-spherical receptacle, with a digitiform internal projection longer or almost the same length of the receptacle (Fig. 9F) and from *A. parana* by the narrow fundus of the spermathecae.

Description of holotype male (M1496). Coloration of cephalothorax, legs, and palpi yellowish brown; abdomen of similar coloration, densely mottled with darker brown markings dorsally and paler ventrally, with some dark spots anterior to the spinnerets. Carapace length 5.17, width 3.91 (Fig. 6A). Abdomen length 5.02, width 1.73. Ocular group length 0.64, width 0.85 (Fig. 6D). Eye sizes and interdistances: AME 0.19, ALE 0.28, PME 0.17, PLE 0.17; AME–AME 0.14, AME–ALE 0.06, PME–PME 0.34, PME–PLE 0.05, ALE–PLE 0.10, AME–PME 0.07. Anterior eye row slightly procurved, posterior row recurved. Clypeus width 0.1. Fovea straight, 0.62 wide. Chelicerae with 8 prolateral denticles and intercheliceral tumescence bearing 7 long, thin setae. Rastellum weak, formed by basally thick setae tapering apically. Labium length 0.78, width 0.79, without cuspules. Maxillae length 1.49, width 0.83, with 18 cuspules on the left and 23 on the right (Fig. 6C). Sternum length 2.89, width 1.93, with three pairs of oval marginal sigilla:

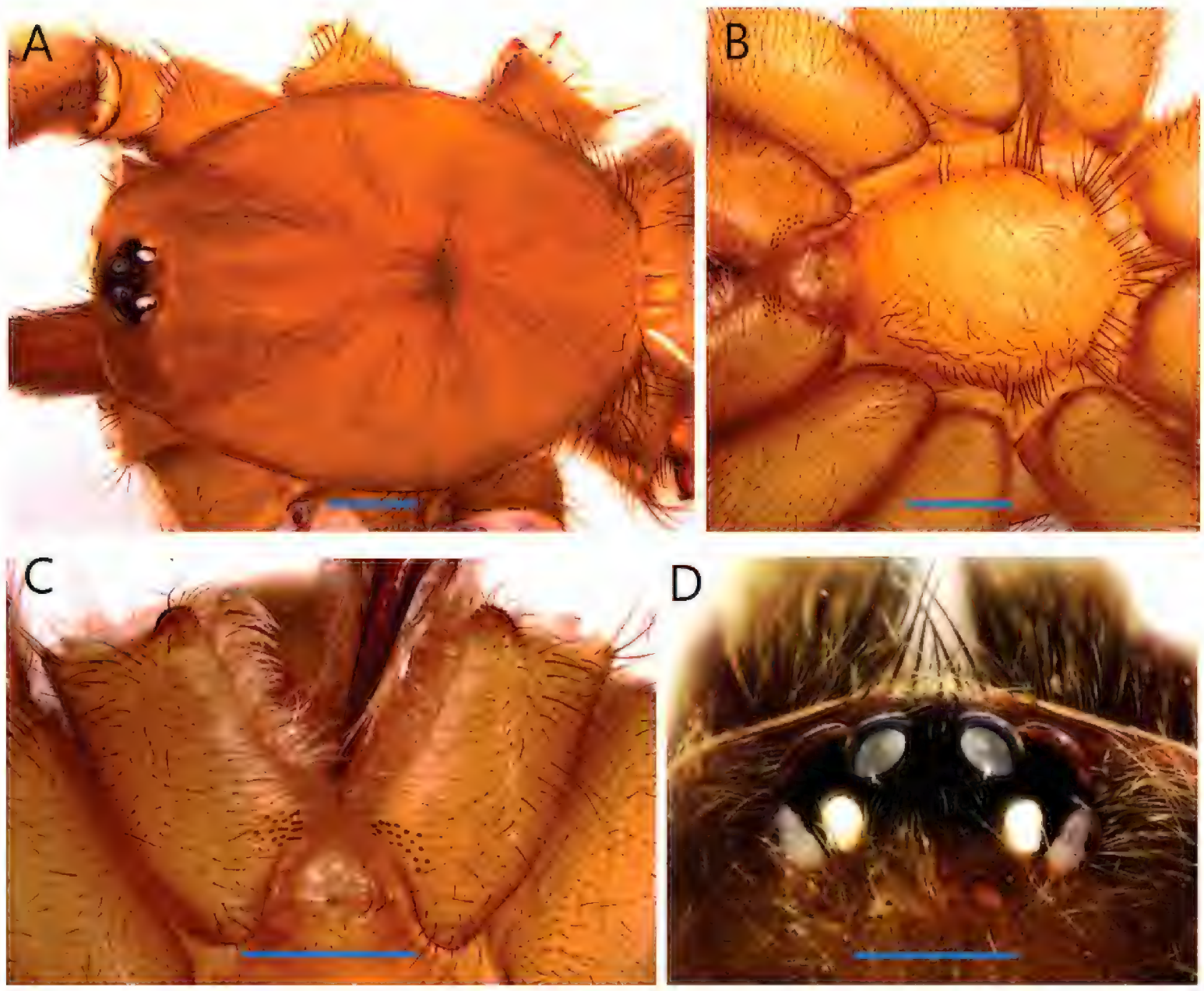

Figure 6. *Acanthogonatus monicae* Signorotto & Ferretti, sp. nov., holotype male (M1496). **A.** Carapace, dorsal view; **B.** Sternum, ventral view; **C.** Labium and maxillae, ventral view. Scale bars: 1 mm.

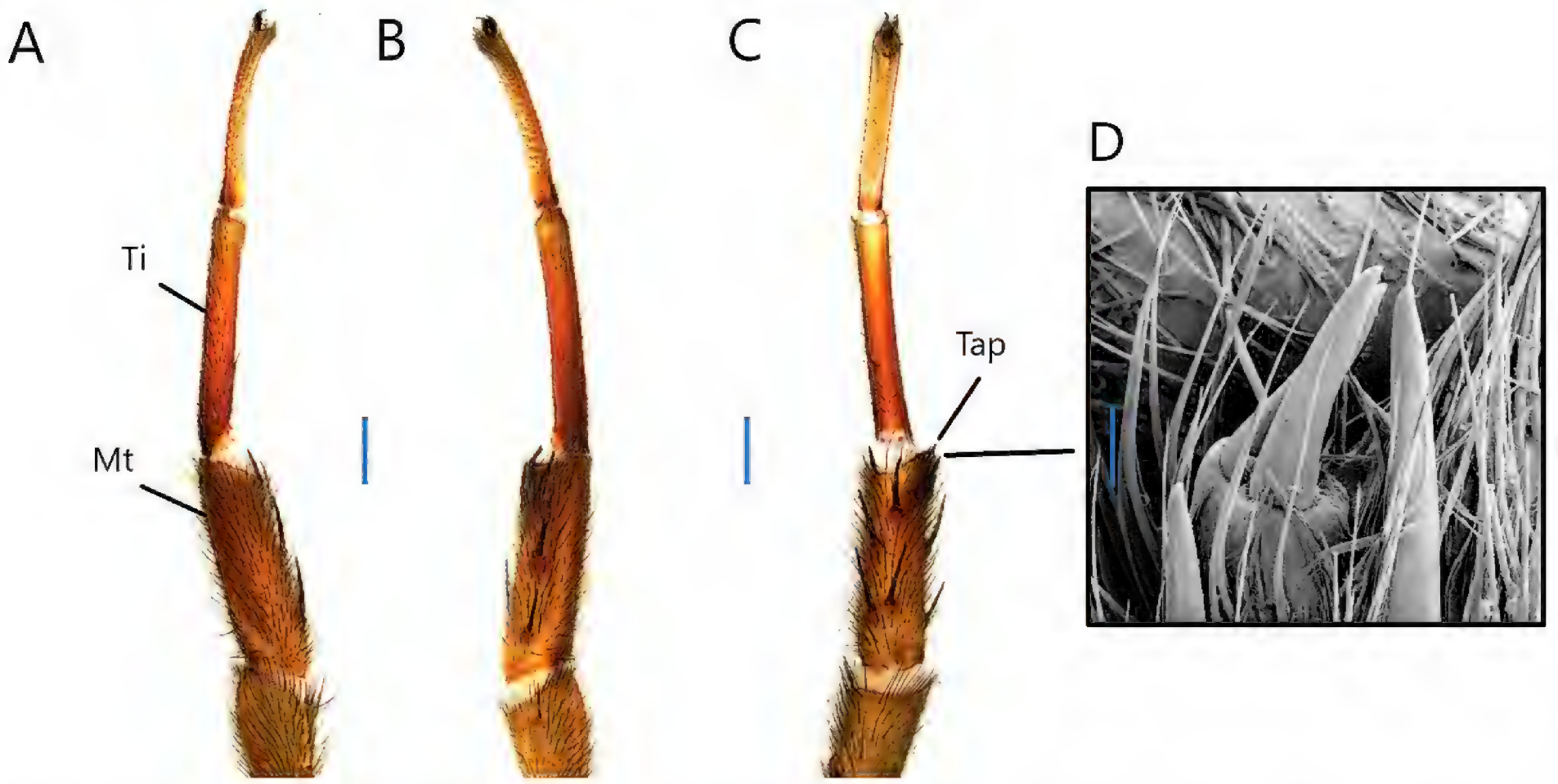

Figure 7. *Acanthogonatus monicae* Signorotto & Ferretti, sp. nov., holotype male (M1496). **A–C.** Patella-Tarsus of leg I. **A.** Prolateral view; **B.** Retrolateral view; **C.** Ventral view; **D.** Detail of tibial apophysis. Abbreviations: Mt, metatarsus; Tap, tibial apophysis; Ti, tibia. Scale bars: 1 mm.

pair I diameter 0.05, distance to margin 0.05; pair II diameter 0.05, distance 0.02; pair III diameter 0.10, distance 0.04 (Fig. 6B). Spinnerets: PMS length 0.41; PLS: basal segment 0.80, median 0.43, apical 0.70. Scopula: leg I, tarsus entire, metatarsus 1/2; leg II, tarsus entire; leg IV, tarsus entire. All tarsi flexible. Tarsal claws with a double row of 9–10 teeth. Leg and palp measurements are shown in Table 3. Tibia I with a well-developed apophysis bearing two short and stout spines (Fig. 7A–C). Spination: palp: femur r 1-0-0, patella 0, tibia r 1-1-0; leg I: femur r 1-0-0, d 2-0-0, patella

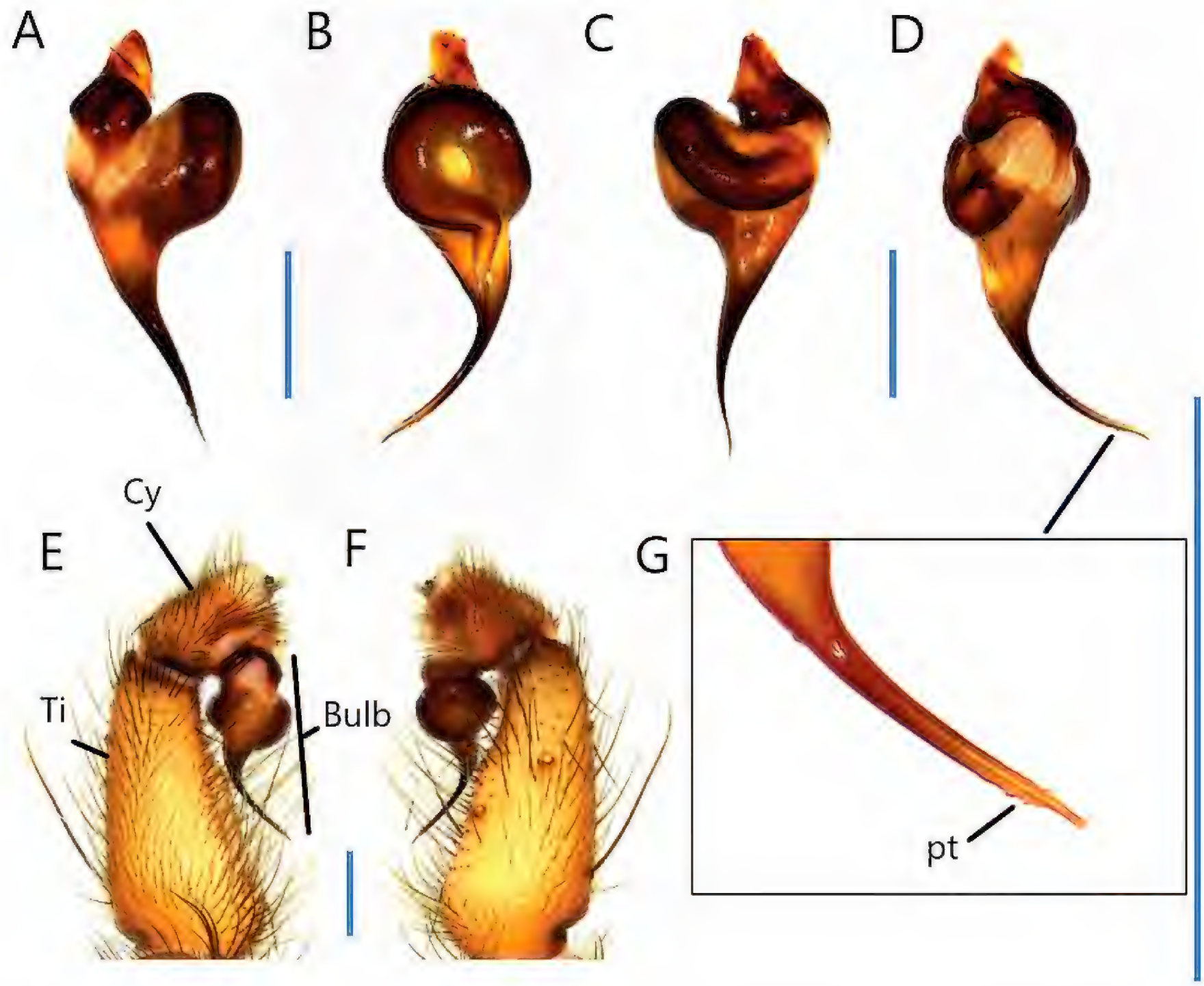

Figure 8. *Acanthogonatus monicae* Signorotto & Ferretti, sp. nov., holotype male (M1496), palpal bulb and palp. **A–D.** Palpal bulb: **A.** Ventral view; **B.** Retrolateral view; **C.** Dorsal view; **D.** Prolateral view. **E–F.** palp: **E.** Prolateral view; **F.** Retrolateral view. **G.** Detail of palpal bulb showing prolateral teeth. Abbreviations: Cy, cymbium; Ti, tibia; pt, prolateral teeth. Scale bars: 1 mm.

r 1-0-0, tibia r 3-1-1, v 1-2-2, metatarsus v 0-1-0; leg II: femur 0, patella 0, tibia r 2-4-3, v 0-1-0, metatarsus r 2-0-0, v 1-0-0; leg IV: femur d 1-0-1, patella r 0-1-1, p 0-1-0, tibia r 0-2-0, p 2-2-0, v 2-1-2, d 1-0-1, metatarsus r 2-0-1, p 2-2-1, v 3-3-2, d 2-3-2. Copulatory organ: bulb pyriform with globose tegulum and long, very thin embolus, straight in dorsal view (Fig. 8A–F), bearing 8–10 subapical teeth (Fig. 8G).

Table 3. Measurements of the legs and palpal segments of the male holotype of *Acanthogonatus monicae*. Note: leg III was missing. All measurements are in millimeters (mm).

	I	II	III	IV	Palp
Femur	4.05	3.02	-	4.49	2.95
Patella	2.25	1.6	-	1.75	1.18
Tibia	2.88	2.36	-	2.91	2.30
Metatarsus	3.02	2.48	-	4.35	-
Tarsus	2.15	2.15	-	2.20	1.10
Total	14.35	11.61	-	15.7	7.53

Description of paratype female (M1498). Color as in male. Carapace length 4.9, width 3.6 (Fig. 9A). Abdomen length 7.8, width 4.9 (Fig. 9C, D). Ocular group length 1.3, width 1.8 (Fig. 9G). Eye sizes and interdistances: AME 0.4, ALE 0.5, PME 0.3, PLE 0.4; AME–AME 0.3, AME–ALE 0.2, PME–PME 0.1, PME–PLE 0.8, ALE–PLE 0.1, AME–PME 0.1. Anterior eye row procurved, posterior row slightly recurved. Clypeus width 0.1. Fovea straight, 0.4 wide. Chelicerae with 7 prolateral denticles. Rastellum weak, formed by basally wide setae tapering apically. Labium length 0.53, width 0.36, without cuspules. Maxillae length 1.9, width 1.14, with 22 cuspules on the left and 24 on the right (Fig. 9E). Sternum length 3.9, width 4.0, with three pairs of marginal oval sigilla: pair I diameter 0.1, distance to margin 0.025; pair II diameter 0.2, distance 0.077; pair III diameter 0.2, distance 0.138 (Fig. 9B). Spinnerets: PMS length 0.9; PLS: basal segment 1.5, median 0.8, apical 0.9. Scopula: leg I, tarsus and metatarsus fully scopulated, entire; leg III and IV, tarsus fully scopulated, entire. Non-flexible tarsi. Legs and palp measurements are shown in Table 4. Tarsal claws with a double row of 7 teeth. Spination: palp: femur 0, patella 0, tibia r 1-0-0, v 2-0-0; leg I: femur d 2-0-0, patella 0, tibia r 2-0-0, metatarsus v 0-0-1; leg III: femur d 2-0-1, patella r 0-1-0, p 1-1-1, d 0-1-0, tibia r 1-1-0, p 2-1-2, v 2-1-1, d 0-2-1,

metatarsus r 2-2-2, p 2-4-3, v 2-2-2, d 2-4-3; leg IV: femur d 1-0-2, patella r 0-1-0, p 0-2-0, tibia r 2-2-1, p 2-1-2, v 3-2-2, d 2-1-0, metatarsus r 2-2-4, p 3-4-3, v 3-2-3, d 2-2-4. Spermathecae with elongate, sub-spherical receptacle with long duct, bearing an internal projection arising from the base of the duct, longer or almost the length of the receptacle (Fig. 9F).

Distribution. Restricted to the Pampean ranges of central Argentina, along the north-central region of Córdoba Province (Fig. 10).

Table 4. Leg and palp measurements of the paratype female of *Acanthogonatus monicae*. Note: leg II was missing in the specimen. Measurements are in mm.

	I	II	III	IV	Palp
Femur	6.2	-	5.3	7.0	4.5
Patella	2.9	-	2.6	3.5	2.4
Tibia	3.7	-	3.0	4.7	2.4
Metatarsus	3.1	-	4.1	6.3	-
Tarsus	2.2	-	2.6	2.6	2.5
Total	18.1	-	17.6	24.1	11.8

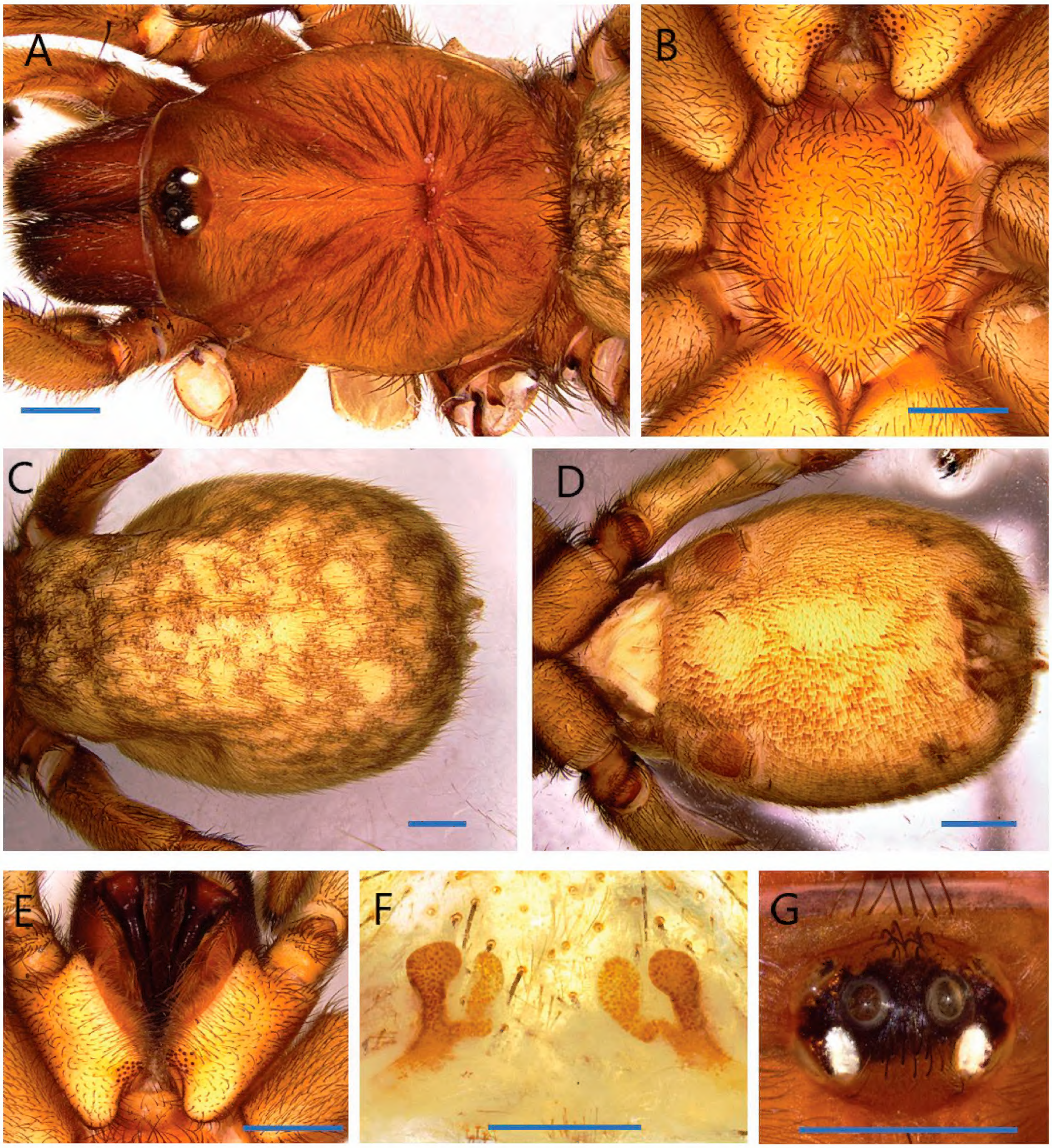

Figure 9. *Acanthogonatus monicae* Signorotto & Ferretti, sp. nov., paratype female (M1498). **A.** Carapace, dorsal view; **B.** Sternum, ventral view; **C.** Abdomen, dorsal view; **D.** Abdomen, ventral view; **E.** Labium and maxillae, ventral view; **F.** Spermathecae, dorsal view; **G.** Eyes, dorsal view. Scale bars: 1 mm.

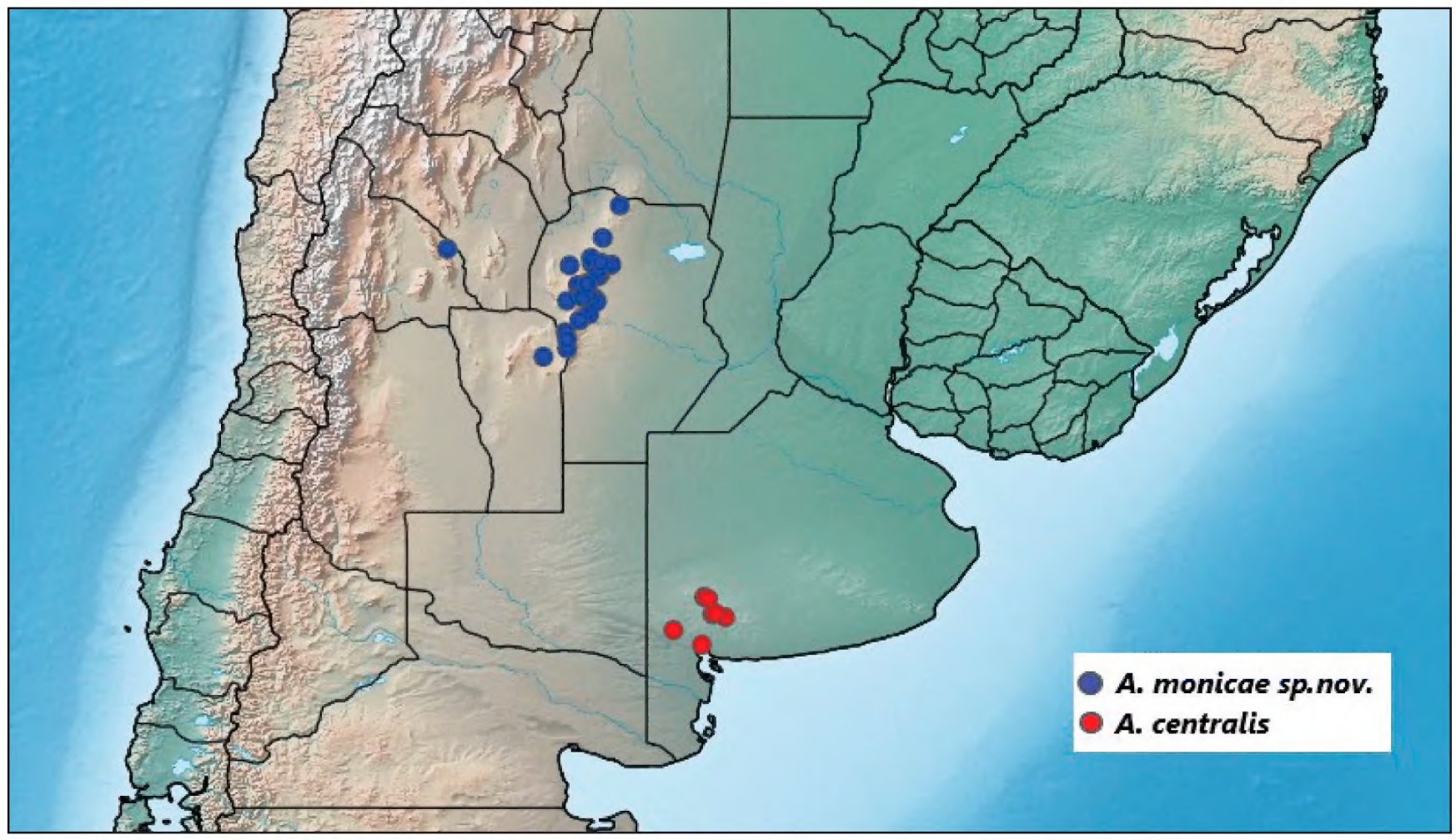

Figure 10. Distribution of *A. monicae* sp. nov. and *A. centralis*. Map showing the known localities after species delimitation, with blue points representing *A. monicae* sp. nov. and red points representing *A. centralis*.

Discussion

Species delimitation in mygalomorph spiders can be a challenging task due to their low morphological variability, evolutionary stasis, and limited dispersal, which lead to high endemism and may result in underestimating diversity through solely morphology-based methods (Goloboff 1995; Hedin and Bond 2006; Ortiz and Francke 2017; Derkarabetian et al. 2019). *Acanthogonatus centralis* exemplifies this, with populations restricted to mountainous regions of Argentina, possibly with absence of gene flow between them (Calatayud-Mascarell et al. 2022). Aggregated dispersal patterns suggested that it might have been a cryptic species complex, morphologically indistinguishable (Pompozzi et al. 2018). Classical morphological traits were to date unclear to establish population limits (Goloboff 1995), but genital differences found in the present study support the hypothesis of distinct lineages, despite little variation in traditional characters (Cooper et al. 2011; Hendrixson et al. 2014; Harvey et al. 2015; Leavitt et al. 2015; Candia-Ramírez and Francke 2020). Similar limitations in morphological diagnosis have been documented in genera such as *Bertmainius* (Migidae) and *Calisoga* (Nemesiidae), where molecular data revealed deeply structured populations hidden by external homogeneity (Harvey et al. 2015; Laevitt et al. 2015).

Molecular species delimitation analyses support two main independent lineages using bPTP, consistent with morphological and also with ecological data. In contrast, ABGD identifies three lineages, splitting Córdoba populations into central (Villa Berna) and northern (Dean Funes) groups. However, ABGD has been shown to overestimate diversity in lineages, such was reported for other mygalomorphs, due to the lack of fixed thresholds, likely caused by strong genetic structuring in sedentary species like *A. centralis* (Hamilton et al. 2014; Leavitt et al. 2015; Candia-Ramírez and Francke 2021; Korba et al. 2022).

Based on actual and historical ecological factors shaping species distributions (Holzmann et al. 2014), we found two disjunct well-defined suitable areas for *A. centralis*. Niche modelling suggests fragmented suitable habitats and gene flow barriers. Although the temperature seasonality (BIO4) was relevant for the predictions of both lineages, Córdoba populations were influenced in high proportion by precipitation related variables (BIO15, BIO19). The predictive models under Pliocene conditions showed two suitable restricted areas for both lineages, and this would be consistent with the divergence times estimated in about 3–5 Ma for the split of two clades, one from Ventania and another one from Pampean ranges in central north Argentina (Calatayud-Mascarell et al. 2022). Thus, this is in agreement with the chance that suitable environments for each lineage were already geographically distinct at that time. These findings reinforce the role of environmental barriers and climatic heterogeneity in promoting divergence and limiting gene flow between these populations.

Based on the integrative evidence from morphological, molecular, and ecological data, we propose the recognition of a new taxon for the Pampean ranges, distributed along the Cordoba Mountain range: *Acanthogonatus monicae* sp. nov. This study not only improves knowledge of the systematics of the family Pycnothelidae in Argentina, but also emphasizes the importance of integrative approaches focused on specific taxa to better understand their diversity and evolutionary relationships. Arguably, these kinds of studies would help to fill both Wallacean (geographic range poorly known) and Linnean (species unknown) shorfalls, thereby providing

essential baseline information for future biodiversity and conservation assessments (Baranzelli et al. 2023).

Competing interests

The authors have declared that no competing interests exist.

Funding

This work was supported by the Consejo Interuniversitario Nacional (CIN) through a fellowship (EVC-CIN), the Agencia I+D+i for supporting the advisor's projects (PICT 2018-1751 and PICT 2021-0407), and the Secretaría General de Ciencia y Tecnología of the Universidad Nacional del Sur (projects PGI 24/ZB87 and 24/ZB00).

Acknowledgements

The authors thank GENETyC for their assistance with molecular analyses, Sofia Copperi, Leonela Schwetdt, and Gabriel Pompozzi for collecting the specimens used in this study, and the Museo Argentino de Ciencias Naturales "Bernardino Rivadavia" (MACN), particularly Martín Ramírez and Cristian Grismado, for their collaboration and for providing images of the type material examined in this study, as well as the author's family for their support throughout her university career.

References

Baranzelli MC, Villalobos F, Cordier JM, Nori J (2023) Knowledge shortfalls' interactions shadow our perception of species' exposure to human threats. Elsevier. Biological Conservation 282: 1–10. https://doi.org/10.1016/j.biocon.2023.110069

Calatayud-Mascarell A, Ferretti N, Enguidanos A, Arnedo MA (2022) Same place, different stories: Disparate evolutionary trends of mygalomorph spiders from the Peripampasic orogenic arc. Journal of Biogeography 49(7): 1234–1247. https://doi.org/10.1111/jbi.14374

Candia-Ramírez DT, Francke OF (2021) Another stripe on the tiger makes no difference? Unexpected diversity in the widespread tiger tarantula Davus pentaloris (Araneae: Theraphosidae: Theraphosinae). Zoological Journal of the Linnean Society 192(1): 75–104. https://doi.org/10.1093/zoolinnean/zlaa107

Catálogo de Arañas de Argentina (2025) Museo Argentino de Ciencias Naturales "Bernardino Rivadavia". Recuperado el 3 de septiembre de 2025. https://sites.google.com/site/catalogodearanasdeargentina/

Chan KO, Hertwig ST, Neokleous DN, Flury JM, Brown RM (2022) Widely used, short 16S rRNA mitochondrial gene fragments yield poor and erratic results in phylogenetic estimation and species delimitation of amphibians. BMC Ecology and Evolution 22(1): 37. https://doi.org/10.1186/s12862-022-01994-y

Cooper SJ, Harvey MS, Saint KM, Main BY (2011) Deep phylogeographic structuring of populations of the trapdoor spider Moggridgea tingle (Migidae) from southwestern Australia: evidence for long-term refugia within refugia. Molecular Ecology 20(15): 3219–3236. https://doi.org/10.1111/j.1365-294X.2011.05160.x

Coyle FA, Ketner ND (1990) Observations on the prey and prey capture behaviour of the funnelweb mygalomorph spider genus Ischnothele (Araneae, Dipluridae). Bulletin of the British Arachnological Society 8(4): 97–104. https://britishspiders.org.uk/node/2648

De Queiroz K (2007) Species concepts and species delimitation. Systematic Biology 56(6): 879–886. https://doi.org/10.1080/10635150701701083

Derkarabetian S, Castillo S, Koo PK, Ovchinnikov S, Hedin M (2019) A demonstration of unsupervised machine learning in species delimitation. Molecular Phylogenetics and Evolution 139: 106562. https://doi.org/10.1016/j.ympev.2019.106562

Ferretti N, Copperi S, Pompozzi G (2014) Fight or flight: agonistic interactions between females of Acanthogonatus centralis Goloboff 1995 (Araneae, Mygalomorphae). Turkish Journal of Zoology 38(3): 354–360. https://doi.org/10.3906/zoo-1304-47

Ferretti N, Pompozzi G, Copperi S, Pérez-Miles F, González A (2012) Mygalomorph spider community of a natural reserve in a hilly system in central Argentina. Journal of Insect Science 12(1): 31. https://doi.org/10.1673/031.012.3101

Ferretti N, Pompozzi G, Pérez-Miles F (2011) Sexual behavior of Acanthogonatus centralis (Araneae: Mygalomorphae: Nemesiidae) from Argentina, with some notes on their burrows. Journal of Arachnology 39(3): 533–536. https://doi.org/10.1636/Hi09-72.1

Goloboff PA (1995) A revision of the South American spiders of the family Nemesiidae (Araneae, Mygalomorphae). Part I: Species from Peru, Chile, Argentina and Uruguay. Bulletin of the American Museum of Natural History 224: 1–189. https://digitallibrary.amnh.org/items/a998e37d-a0e5-4d7d-b40a-1dc3566a7870

Hamilton CA, Hendrixson BE, Bond JE (2016) Taxonomic revision of the tarantula genus Aphonopelma Pocock, 1901 (Araneae, Mygalomorphae, Theraphosidae) within the United States. ZooKeys 560: 1–340. https://doi.org/10.3897/zookeys.560.6264

Harvey MS, Rix MG, Framenau VW, Hamilton ZR, Johnson MS, Teale RJ, Humphreys G, Humphreys WF (2015) Refugia within refugia: In situ speciation and conservation of threatened Bertmainius (Araneae: Migidae), a new genus of relictual trapdoor spiders endemic to the mesic zone of south-western Australia. Invertebrate Systematics 29(6): 511–553. https://doi.org/10.1071/IS15024

Hedin M, Bond JE (2006) Molecular phylogenetics of the spider infraorder Mygalomorphae using nuclear rRNA genes (18S and 28S): Conflict and agreement with the current system of classification. Molecular Phylogenetics and Evolution 41(2): 454–471. https://doi.org/10.1016/j.ympev.2006.05.017

Hendrixson BE, Guice AV, Bond JE (2015) Integrative species delimitation and conservation of tarantulas (Araneae, Mygalomorphae, Theraphosidae) from a North American biodiversity hotspot. Insect Conservation and Diversity 8(2): 120–131. https://doi.org/10.1111/icad.12089

Hertwig S, De Sá RO, Haas A (2004) Phylogenetic signal and the utility of 12S and 16S mtDNA in frog phylogeny. Journal of Zoological Systematics and Evolutionary Research 42(1): 2–18. https://doi.org/10.1111/j.1439-0469.2004.00225.x

Holzmann I, Agostini I, DeMatteo K, Areta JI, Merino ML, Di Bitetti MS (2015) Using species distribution modeling to assess factors that determine the distribution of two parapatric howlers (Alouatta spp.) in South America. International Journal of Primatology 36: 18–32. https://doi.org/10.1007/s10764-014-9805-1

Indicatti RP, Folly-Ramos E, Vargas AB, Lucas SM, Brescovit AD (2015) Two new tiny Nemesiidae species from Reserva Biológica do Tinguá, Rio de Janeiro, Brazil (Araneae: Mygalomorphae). Zoologia (Curitiba) 32(2): 123–138. https://doi.org/10.1590/S1984-46702015000200003

Jezkova T, Olah-Hemmings V, Riddle BR (2011) Niche shifting in response to warming climate after the last glacial maximum: inference from genetic data and niche assessments in the chisel-toothed kangaroo rat (Dipodomys microps). Global Change Biology 17(11): 3486–3502. https://doi.org/10.1111/j.1365-2486.2011.02508.x

Korba J, Opatova V, Calatayud-Mascarell A, Enguídanos A, Bellvert A, Adrián S, Sánchez-Vialas A, Arnedo MA (2022) Systematics and phylogeography of western Mediterranean tarantulas (Araneae: Theraphosidae). Zoological Journal of the Linnean Society 196(2): 845–884. https://doi.org/10.1093/zoolinnean/zlac042

Lanfear R, Hua X, Warren DL (2016) Estimating the effective sample size of tree topologies from Bayesian phylogenetic analyses. Genome Biology and Evolution 8(8): 2319–2332. https://doi.org/10.1093/gbe/evw171

Leavitt DH, Starrett J, Westphal MF, Wong HT, Hedin M (2015) Multilocus sequence data reveal dozens of putative cryptic species in a radiation of endemic Californian mygalomorph spiders (Araneae, Mygalomorphae, Nemesiidae). Molecular Phylogenetics and Evolution 91: 56–67. https://doi.org/10.1016/j.ympev.2015.05.016

Lima-Ribeiro MS, Varela S, González-Hernández J, De Oliveira G, Diniz-Filho JAF, Terribile LC (2015) EcoClimate: A database of climate data from multiple models for past, present, and future for macroecologists and biogeographers. Biodiversity Informatics 10: 1–9. https://doi.org/10.17161/bi.v10i0.4955

Montes de Oca L, Indicatti RP, Opatova V, Almeida M, Pérez-Miles F, Bond JE (2022) Phylogenomic analysis, reclassification, and evolution of South American nemesioid burrowing mygalomorph spiders. Molecular Phylogenetics and Evolution 168: 107377. https://doi.org/10.1016/j.ympev.2021.107377

Nguyen NK, Nguyen PB, Nguyen HT, Le PH (2015) Screening the optimal ratio of symbiosis between isolated yeast and acetic acid bacteria strain from traditional kombucha for high-level production of glucuronic acid. LWT-Food Science and Technology 64(2): 1149–1155. https://doi.org/10.1016/j.lwt.2015.07.018

Opatova V, Hamilton CA, Hedin M, Montes de Oca L, Král J, Bond JE (2019) Phylogenetic systematics and evolution of the spider Infraorder Mygalomorphae using genomic scale data. Systematic Biology 69(4): 671–707. https://doi.org/10.1093/sysbio/syz064

Ortiz D, Francke OF (2017) Reconciling morphological and molecular systematics in tarantulas (Araneae: Theraphosidae): Revision of the Mexican endemic genus Bonnetina. Zoological Journal of the Linnean Society 180(4): 819–886. https://doi.org/10.1093/zoolinnean/zlw013

Pearson RG, Raxworthy CJ, Nakamura M, Peterson AT (2007) Predicting species distributions from small numbers of occurrence records: A test case using cryptic geckos in Madagascar. Journal of Biogeography 34: 102–117. https://doi.org/10.1111/j.1365-2699.2006.01594.x

Petrunkevitch A (1925) Descriptions of new or inadequately known American spiders. Annals of the Entomological Society of America 18(3): 313–323. https://doi.org/10.1093/aesa/18.3.313

Phillips SJ, Dudik M, Schapire RE (2009) MAXENT (Maximum Entropy Modeling of Species Geographic Distributions). Version 3.3.3k. http://www.cs.princeton.edu/~schapire/maxent/

Pompozzi G, Copperi S (2018) Feeding frequency, prey acceptance, and natural diet of the mygalomorph spider Acanthogonatus centralis Goloboff 1995 (Araneae: Nemesiidae). Zoological Studies 57: 1–10. https://doi.org/10.6620/ZS.2018.57-31

Raven RJ (1985) The spider infraorder Mygalomorphae (Araneae): Cladistics and systematics. Bulletin of the American Museum of Natural History 182: 1–180. http://hdl.handle.net/2246/955

Rockney HJ, Porcino N, Leache AD, Ofori-Boateng C (2015) A comparison of DNA barcoding markers in West African frogs. African Journal of Herpetology 64(2): 135–147. https://doi.org/10.1080/21564574.2015.1114530

Ronquist F, Huelsenbeck JP (2003) MrBayes 3: Bayesian phylogenetic inference under mixed models. Bioinformatics 19(12): 1572–1574. https://doi.org/10.1093/bioinformatics/btg180

Vences M, Nagy ZT, Sonet G, Verheyen E (2012) DNA barcoding amphibians and reptiles. In: DNA barcodes: Methods and protocols. Humana Press, Totowa, NJ, 79–107. https://doi.org/10.1007/978-1-61779-591-6_5

Warren DL, Glor RE, Turelli M (2010) ENMTools: A toolbox for comparative studies of environmental niche models. Ecography 33(3): 607–611. https://doi.org/10.1111/j.1600-0587.2009.06142.x

World Spider Catalog (2025) World Spider Catalog. Version 26. Natural History Museum Bern. [accessed on 5 September 2025] https://doi.org/10.24436/2

Xia Y, Gu HF, Peng R, Chen Q, Zheng YC, Murphy RW, Zeng XM (2012) COI is better than 16S rRNA for DNA barcoding Asiatic salamanders (Amphibia: Caudata: Hynobiidae). Molecular Ecology Resources 12(1): 48–56. https://doi.org/10.1111/j.1755-0998.2011.03055.x

Zhang J, Kapli P, Pavlidis P, Stamatakis A (2013) A general species delimitation method with applications to phylogenetic placements. Bioinformatics 29(22): 2869–2876. https://doi.org/10.1093/bioinformatics/btt499